Journal of Foraminiferal Research, v. 54, no. 2, p. 172–187, April 2024

HOLOCENE FORAMINIFERA, CLIMATE, AND DECELERATING RISE IN SEA LEVEL ON THE MUD PATCH, SOUTHERN NEW ENGLAND CONTINENTAL SHELF

KENNETH G. MILLER[1,*], JAMES V. BROWNING[1], LLOYD D. KEIGWIN[2], JASON D. CHAYTOR[3], EMILY R. SCHNEIDER[1], MATTHEW RICHTMYER[1] AND W. JOHN SCHMELZ[1]

ABSTRACT

We examined Holocene benthic foraminiferal biofacies, % planktonic foraminifera, and lithofacies changes from New England mud patch cores and present a relative sea-level (RSL) record to evaluate evolution of these rapidly deposited (30–79 cm/kyr) muds. Sandy lower Holocene sections are dominated by *Bulimina marginata*. The mud patch developed from 11–9 ka as RSL rise slowed from 10 to 7 mm/yr; mud deposition began when the cores (69 to 91 m modern) were inundated below storm wave base. An *Elphidium-B. marginata* fauna developed at ca. 7–6 ka as RSL rise slowed from approximately 7 to 2 mm/yr. A *Globobulimina* fauna developed at 3 ka as RSL rise slowed to 1 mm/yr, reflecting lower O_2 conditions. Single specimen $\delta^{18}O$ analyses of *Globobulimina* show ~1‰ variations over the past 3 kyr, reflecting a shelf bottom water seasonal cycle of 4–5°C, and a temperature minimum during the Little Ice Age with warming since.

BACKGROUND

INTRODUCTION

The broad continental shelf of the U.S. east coast in the mid-Atlantic Bight (MAB; defined as extending from the Nantucket Shoals to Cape Hatteras; Bumpus, 1973), is dominated by sand sheets and sand ridges (e.g., Swift et al., 1973). The modern U.S. Atlantic continental shelf has low sediment input, and previous studies have suggested this is because sediment is trapped in estuaries (summary in Miller et al., 2014). Studies of surface grab samples have shown that MAB surface shelf deposits are almost exclusively sand (>63 mm; Hollister, 1973; Williams et al., 2007) except for the region south of Cape Cod, Massachusetts. Thus, modern sediments fail to follow the classic graded shelf model of progressive fining offshore (Swift et al., 1971), with sand grading to mud on the middle shelf (e.g., below storm wave base of 30–50 m; Grant, 2019). Instead, the complete dominance of sands prompted Emery (1968) to classify modern shelf sedimentation on this region as "relict", a product of the Holocene transgression, and not in equilibrium with modern shelf processes. Swift et al. (1971) recognized that the "relict" sands were initially deposited as shoreface sediments now residing in various water depths across the shelf, but they subsequently have been redeposited in modern hydrodynamic equilibrium and applied the term "palimpsest". More recent studies have shown that not all mud is trapped in estuaries; abundant mud is supplied during floods from major rivers (e.g., Hudson River), but the muds are entrained, swept across the shelf, and settle onto the continental slope (Glenn et al., 2007), which is in fact graded from sand to silt to clay (Miller & Lohmann, 1982).

The notable exception to the paucity of mud in the MAB is the New England mud patch (NEMP; Fig. 1) south of Cape Cod, where rapidly deposited Holocene sandy muds accumulate (Twichell et al., 1977, 1981; Bothner et al., 1981; Goff et al., 2019; Chaytor et al., 2022). Holocene sandy muds to muddy sands in the NEMP are concentrated in this area on antecedent sand ridges by shelf currents and accumulate at high rates (>30 cm/kyr; e.g., Bothner et al., 1981; Chaytor et al., 2022; Goff et al., 2019; Twichell et al., 1977; Twichell et al., 1981) providing high-resolution records of climate and sea-level change. Previous studies of the NEMP have focused on acoustic imaging and lithologies and geochemistry of cores taken in the NEMP (Bothner et al., 1981; Chaytor et al., 2022; Goff et al., 2019; Twichell et al., 1977; Twichell et al., 1981). Here we use foraminiferal biofacies and lithofacies changes in Holocene cores from the NEMP to interpret the evolution of the mud patch in response to relative sea-level (RSL) rise.

Benthic foraminiferal faunas are often used as paleobathymetric indicators (e.g., Bandy & Arnal, 1960; Natland, 1933) and to assess paleoenvironmental parameters (e.g., organic carbon, carbonate saturation, or substrate). Bandy & Arnal (1960) suggested that benthic foraminifera have distinct upper and lower depth limits, though subsequent studies have emphasized that benthic foraminifera are correlated to water-mass properties (Schnitker, 1974; Streeter, 1973), organic carbon/food availability (Gooday, 1988; Miller & Lohmann, 1982), and carbonate saturation (Bremer & Lohmann, 1982), which may vary independently of depth. Nevertheless, benthic foraminifera from paleoshelves provide evidence for water depth and relative sea-level changes (e.g., Katz et al., 2013).

Previous benthic foraminiferal studies in the region include a long history of studies of samples from the MAB continental shelf (Buzas & Culver, 1980; Culver & Buzas, 1980; Gevirtz et al., 1971; Murray, 1973; Parker, 1948; Poag et al., 1980) and slope (Cushman, 1918; Miller & Lohmann, 1982). The type specimen of one of the most widely used benthic species, *Uvigerina peregrina* Cushman, was taken on the continental slope south of Cape Cod (Miller & Lohmann, 1982). Shelf foraminifera from the MAB show a typical generic predominance biofacies progressing from *Elphidium* spp. in the inner-middle neritic zone (<45 m), to *Saccammina* (northern MAB) or *Cibicidoides* (southern MAB) in the middle neritic zone (~45–100 m), to *Bulimina-Cassidulina* in the outer neritic zone (100–200 m; Poag et al., 1980). Even on the sand-dominated ridges, different benthic foraminiferal faunas live in troughs versus ridge crests since the slightly muddy trough substrates contain higher organic carbon, higher foraminiferal abundances, and higher foraminiferal diversity (Culver & Snedden, 1996; Poag et al., 1980).

[1] Department of Earth & Planetary Sciences, Rutgers University, 610 Taylor Road, Piscataway, NJ 08540
[2] Department of Marine Geology and Geophysics, 266 Woods Hole Road, MS #8, Woods Hole Oceanographic Institution, Woods Hole, MA 02543
[3] United States Geological Survey, 384 Woods Hole Road, Woods Hole, MA 02543
* Correspondence author. E-mail: kgm@rutgers.edu

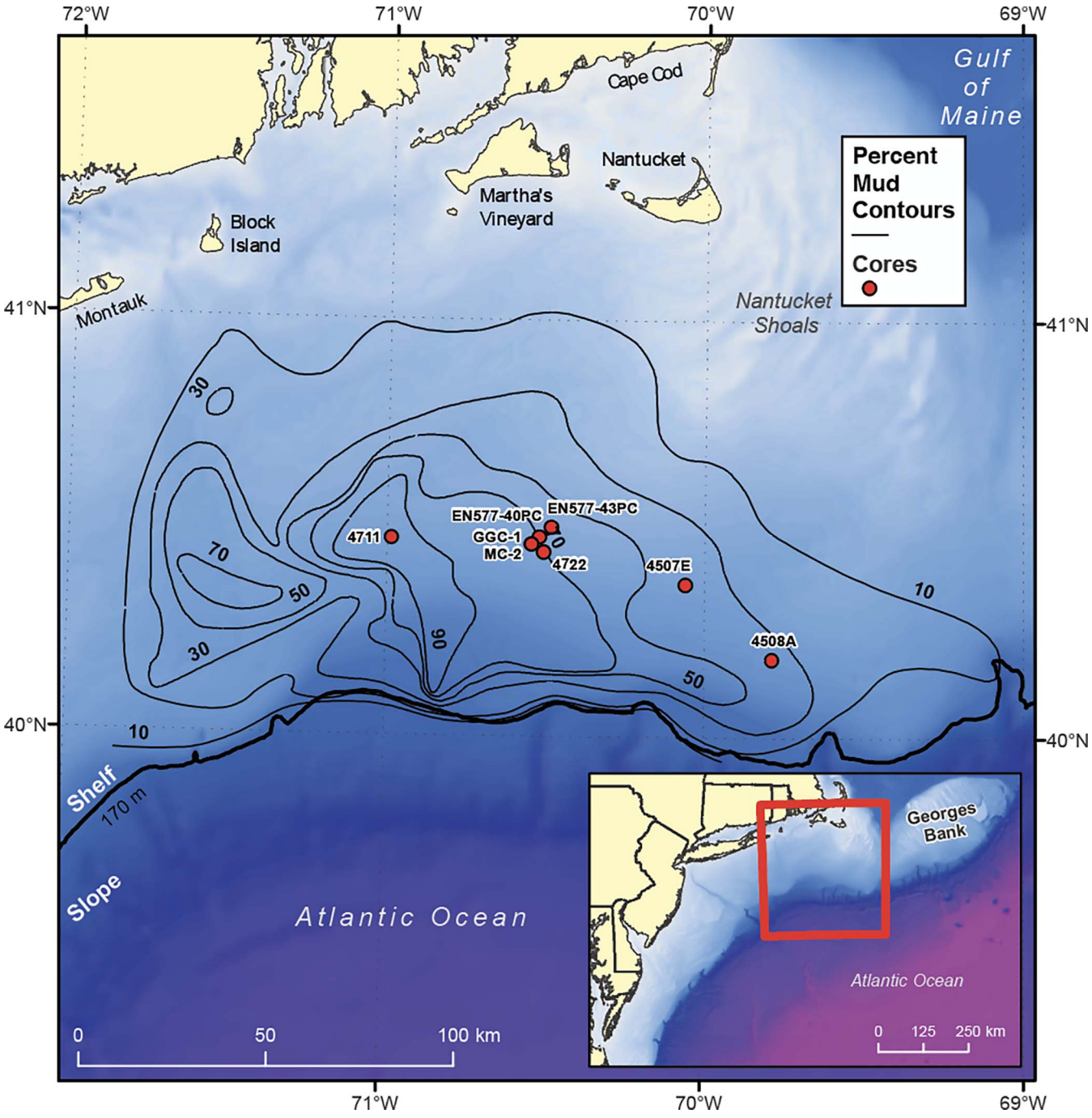

FIGURE 1. Bathymetric location map of the New England Mud Patch (NEMP). Thin black lines indicate percent mud in surface sediments that define the mud patch after Bothner et al. (1982). The shelf-slope break is approximated by the 170-m isobath (thick black line). Cores examined here are red circles. Inset map shows the mid-Atlantic Bight (purple = >3000 m water depth) and red box indicates location of large map.

Our objective in this contribution is to evaluate the evolution of Holocene (last 11,700 years) mud accumulation and environmental changes on the modern continental shelf using foraminifera (benthic foraminiferal biofacies and percent planktonic foraminifera of total foraminifera), grain size, and stable isotopic analyses. We specifically want to address why and under what conditions mud deposition initiated on the New England continental shelf, contrasting with sand sheet and ridge deposition in other parts of the MAB. To do this, we construct a RSL record for this region to evaluate effects of the deglacial rise on depositional environments and foraminiferal biofacies. In addition, differing sub-environments in the NEMP provide specific tests of controls on benthic foraminiferal biofacies. Specific questions are:

1) How do benthic foraminiferal biofacies in the mud patch differ from their distribution in the Holocene sand sheet and ridges that comprise most of the modern U.S. continental shelf (Gevirtz et al., 1971; Poag et al., 1980)?

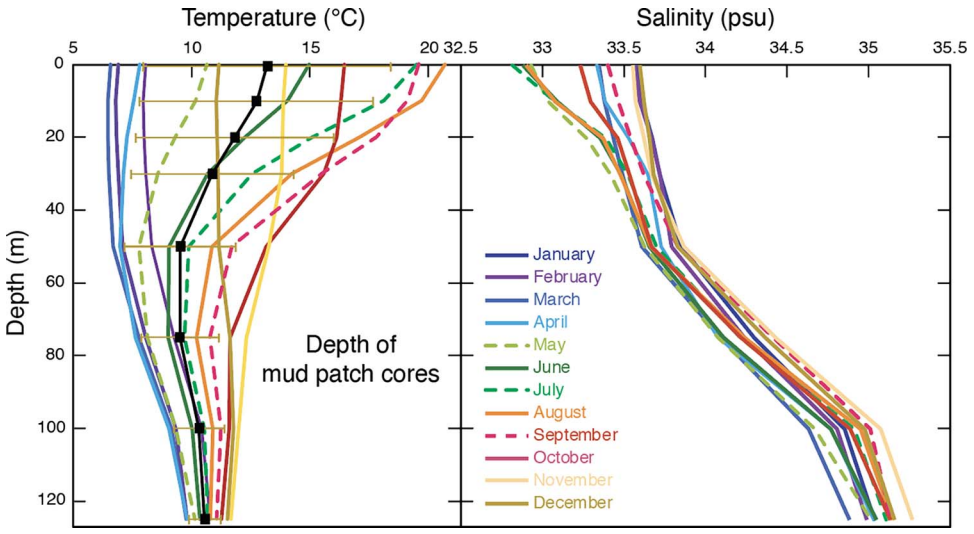

FIGURE 2. Monthly and annual temperature and salinity profiles for the NEMP. Data from NODC (Levitus) World Ocean Atlas 1994 (https://psl.noaa.gov/data/gridded/data.nodc.woa94.html). Temperature range for a mean annual temperature (black line with boxes) is shown with one sigma deviation error bar. Colors correspond to months.

2) How similar are benthic foraminiferal biofacies in the mud patch to the organic-rich lithologies on the adjacent continental shelf and slope (Miller & Lohmann, 1982)?
3) How do benthic foraminiferal biofacies compare between organic-poor (core 4507) and moderately organic-rich cores deposited under similar water depths?
4) How was the oceanographic evolution of the shelf affected by the decreasing rate of rise in sea level during the Holocene?

HYDROGRAPHY

NEMP hydrographic data were taken from National Oceanographic Data Center (NODC) Levitus World Ocean Atlas 1994 (https://psl.noaa.gov/data/gridded/data.nodc.woa94.html). Seasonal range at the surface is from 6.5 to 20.5°C and 32.7 to 33.6 practical salinity units [psu; at the depth of the cores the seasonal ranges are attenuated (7–12.5°C; ~34 psu; Fig. 2)].

The NEMP is in the northern reaches of the MAB. Water masses in the MAB consist of relatively fresh Shelf Water (salinities <35 psu), more saline Slope Water (35–36 psu), and the warm (>18°C), salty (>36 psu) Gulf Stream Water that flows in the western North Atlantic (Beardsley & Boicourt, 1981). The front between Shelf and Slope Water is not rigidly fixed to the shelf/slope break, which lies in this region at 160–170 m (Uchupi, 1968). The source of Slope Water has been attributed to the Labrador Current, although it is more likely locally derived through winter cooling (Beardsley & Boicourt, 1981). A cyclonic gyre (counterclockwise) of northeast-flowing Slope Water and southwest-flowing Shelf Water is geostrophically balanced by regional wind forcing, although the processes controlling the position and movement of the boundary between Shelf and Slope waters are poorly understood (Beardsley & Boicourt, 1981). Gulf Stream eddies (warm core rings) advect warm, salty water to the region. Intrusions of warm core rings occur on the continental shelf in this region (Zhang & Gawarkiewicz, 2015).

Initial general circulation studies of the continental shelf in and around the NEMP suggested predominant flow from the NE to SW (Bumpus, 1973; Mazzullo et al., 1988). Circulation velocities on MAB shelf have been well defined recently by decadal (2007–2016) hourly resolution maps of the surface currents generated by a regional-scale high frequency Radar network (Roarty et al., 2019). The maps show general flow from the NE to SW with a mean flow in excess of 8 cm/s on the MAB outer continental shelf. The exception to this is the region of the NEMP where velocities are generally less than 4 cm/s (Roarty et al., 2019). The present-day velocity minimum explains the preservation of mud, which is otherwise swept off the shelf in other parts of the MAB.

The main thermocline and oxygen minimum zone in this region are shallow and seasonably stable (<400 m; Miller & Lohmann, 1982). Dissolved oxygen in the water column remains moderate, even in the oxygen minimum zone (>3 mL/L; >134 mmol/L). Though shelf waters are generally well oxygenated, seasonal hypoxia occurs in summer in the MAB on the shelf in response to upwelling (Glenn et al., 2004), where hypoxia is less than approximately 2 m/L (<89 mmol/L; Vaquer-Sunyer & Duarte, 2008).

METHODS

Sediment samples for foraminiferal biofacies and lithofacies analysis were obtained from two generations of NEMP Vibracores and piston cores (Fig. 1) taken by the USGS [Cruise FY005 (Bothner et al., 1981); and 2017 Seabed Characterization Experiment; Cruise EN577 (Chaytor et al., 2022)] and archived at the USGS Woods Hole Coastal and Marine Science Center's Samples Repository. Approximately 20-cm^3 sized samples were obtained every 25–30 cm from cores from Bothner et al. (1981): Vibracore 4507 (91 m water depth; 0.5% total organic content [TOC]; 32 cm/kyr sedimentation rate); Vibracore 4508 (82 m water depth; 0.8% TOC, 47 cm/kyr); Vibracore 4711 (81 m, 39 cm/kyr); and Vibracore 4722 (79 m water depth; 73 cm/kyr; Figs. 3–6). Values of TOC were reported for cores 4507 and 4508 by Bothner et al. (1981) but were not reported for cores 4711 and 4722; however, gravity core 4712 next to core 4711 had high TOC (1.9%;

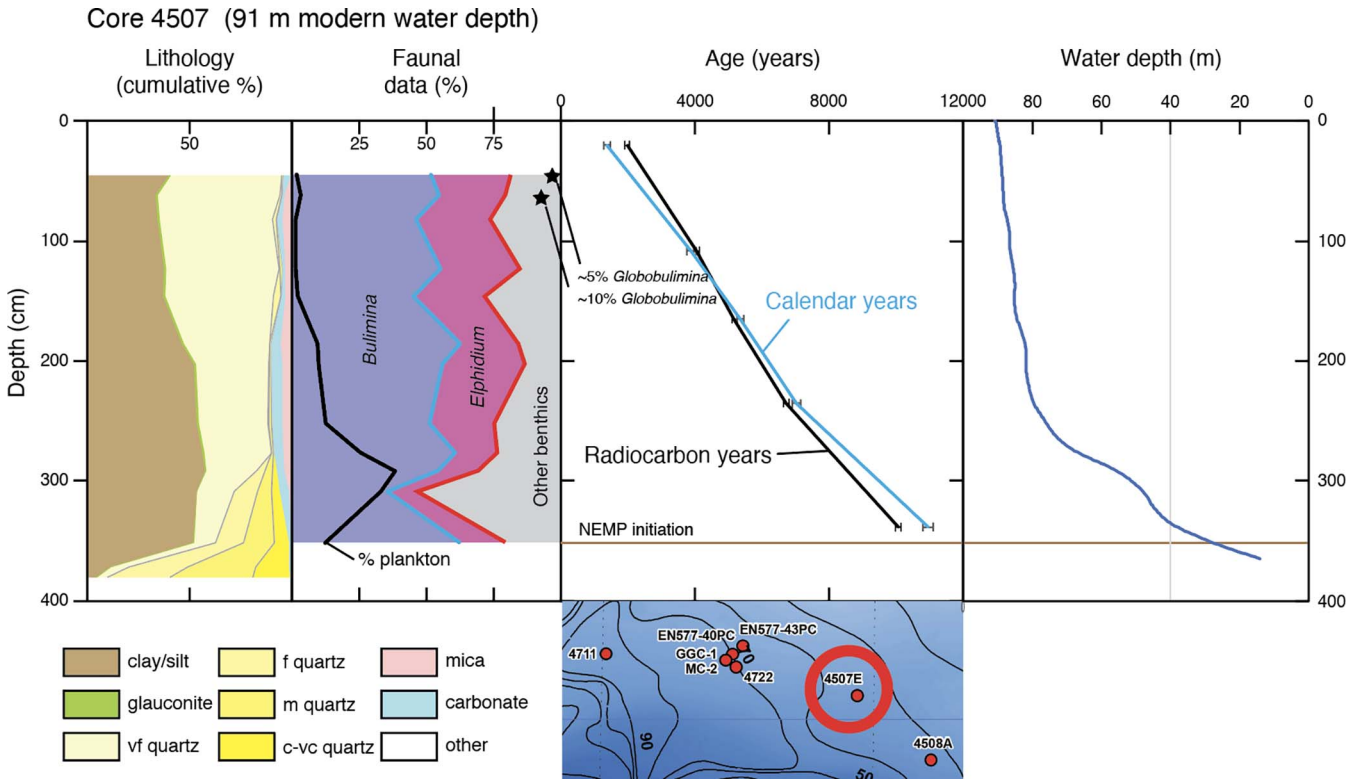

FIGURE 3. Cumulative percentage of lithology, cumulative percentage of benthic foraminiferal generic biofacies, percent planktonic foraminifera of total foraminifera (black line), and ages (black = radiocarbon years; blue = calendar years) plotted versus depth in Vibracore 4507. Inset map shows core locations with 4507 circled. Legend shows lithologies: vf = very fine sand, f = fine sand, m = medium sand, c-vc = coarse to very coarse sand. Water depth (m) estimates were derived by differencing our southern Massachusetts RSL from current water depth.

Bothner et al., 1981). Thus, cores 4507 and 4711 provide a low vs. high TOC comparison.

Seven and nine samples were taken from more recently obtained piston cores EN577-43PC (69 m water depth) and EN577 40PC (74 m water depth; Boggess et al., 2021; Chaytor et al., 2022), respectively at 50–100 cm intervals (Figs. 7, 8). These samples were obtained to evaluate post-archiving dissolution of benthic foraminifera suggested by comparison of our preliminary data from Vibracores (Bothner et al., 1981) with that of Chaytor et al. (2022), and because of their radiocarbon chronology (Table 1).

Each sample was oven dried (<50°C) and weighed before washing and then washed to remove mud content (silt and clay, <63 mm size fraction), preserving the sand fraction that contains microfossils including foraminifera. Cumulative percent plots of lithologies were computed from washed samples, and the dry weight was used to compute the percentage of sand. The sand fraction was dry sieved through 125-, 250-, and 500-µm sieves, and the fractions were weighed to obtain the percent of very fine, fine, medium, and coarse-very coarse sand. The sand fractions were examined using a microscope, and a visual estimate was made of the relative percentages of quartz, glauconite, carbonate (foraminifers and other shells), mica, and other materials by comparison to standard estimates (Rothwell, 1989). The lithologies are displayed on cumulative percentage plots (Figs. 3–8), which provide a visual means of evaluating vertical trends.

Foraminifera larger than 150 µm were picked from aliquots and identified to species level, and population data were recorded as counts (Table A1) and presented as cumulative percentage plots (Figs. 3–8). Taxonomy follows Parker (1948), Barker (1960), and Poag et al. (1980). We chose this fraction to be consistent with most previous benthic foraminiferal census studies (e.g., Streeter, 1973), though some studies have evaluated larger (>250 µm, Miller & Lohmann, 1982; Chaytor et al., 2022) or finer (>125 µm, Schnitker, 1974; >63 µm, Culver & Snedden, 1996) size fractions. While we lose information obtainable from the 63–150-µm size fraction, we gain information on larger taxa (i.e., in an aliquot picked from the >63-µm size fraction, many larger taxa are underemphasized, while small, difficult-to-identify taxa are emphasized). The larger size fraction (>250 µm) also reveals similar trends but tends to emphasize larger taxa (e.g., *Globobulimina*; Chaytor et al., 2022).

Samples from Woods Hole Oceanographic Cruise *Oceanus* 326 Core GGC-1-1-1 (40.4605°N, 70.5448°W, 339 cm length, 80 m water depth; https://maps.ngdc.noaa.gov/viewers/imlgs/samples/table?repository=WHOI&platform=Oceanus&device=core%2C+gravity&cruise=OCE326) in the NEMP (Fig. 1) were analyzed for $\delta^{18}O$ (Table A2, Fig. 9) to constrain temperature and $\delta^{18}O_{seawater}$ variations. Using standard methods (Keigwin, 2004), we generally made four measurements every 1 cm on *Globobulimina affinis* from the >250-µm size fraction from GGC-1 (Table A2). Results are presented as the mean value with error bars showing the standard error of the mean. Analytical error is less than 0.1‰.

Age control is provided by radiocarbon dating. Radiocarbon ages from Bothner et al. (1981), Chaytor et al. (2022), and Oc326 Core GGC-1-1-1 (reported here) were calibrated to calendar years using Marine20 radiocarbon calibration curves (Heaton et al.,

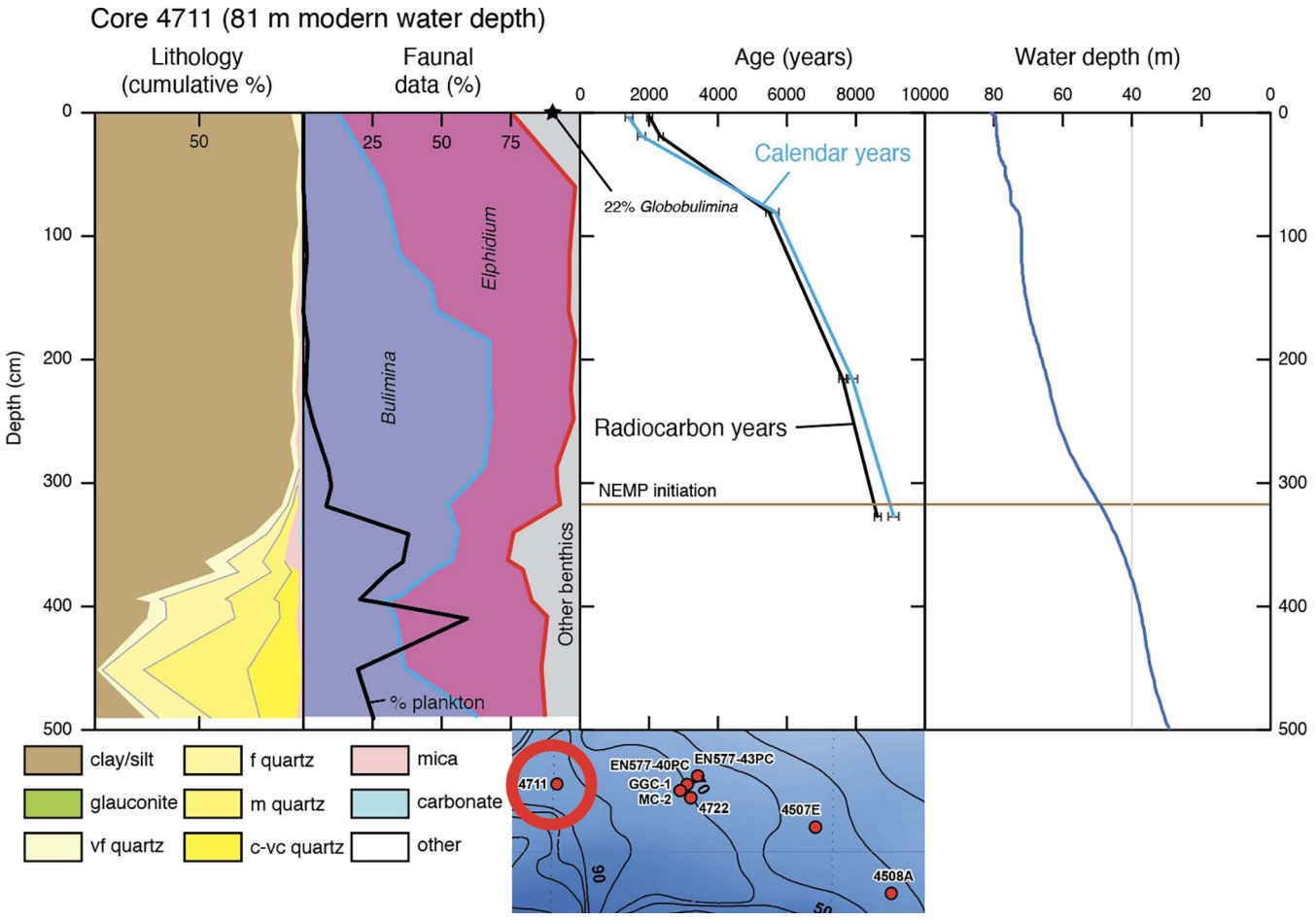

FIGURE 4. Cumulative percentage of lithology, cumulative percentage of benthic foraminiferal biofacies, percent planktonic foraminifera of total foraminifera (black line), and ages (black = radiocarbon years; blue = calendar years) plotted versus depth in Vibracore 4711. Inset map shows core locations with 4711 circled. Legend shows lithologies: vf = very fine sand, f = fine sand, m = medium sand, c-vc = coarse to very coarse sand. Water depth (m) estimates were derived by subtracting our southern Massachusetts RSL estimates from current water depths.

2020; Table 1, Figs. 3–9). We report radiocarbon dates in years before 1950 Common Era (e.g., 10,070 yr) and discuss calendar years in kiloyears before present rounded to 0.1 kyr (e.g., 10.1 ka; Table 1).

Relative sea level data for the southern Massachusetts continental shelf were compiled by Engelhart & Horton (2012. The data are categorized by index points (boxes; Fig. 10) that have a known range of water depths, terrestrial limiting dated levels that provide an upper limit on the position of RSL (inverted Ts, Fig. 10), and marine limiting dated levels that formed below mean tide level and provide a lower limit on the position of RSL (Ts, Fig. 10). Therefore, reconstructed RSL must fall below freshwater limiting dates and above marine limiting dates (Fig. 10).

To obtain a RSL curve using the southern Massachusetts index and limiting points, we applied a Bayesian hierarchical model with Gaussian process priors (Ashe et al., 2019; Rasmussen & Williams, 2006) to estimate RSL variation in southern Massachusetts over the past 12,000 years. To construct this model, we used primary sources of data: 1) the Engelhart & Horton (2012) database, comprised of U.S. East Coast RSL measurements; 2) a Global Mean Sea Level (GMSL) record covering the last 30,000 years generated by Lambeck et al. (2014) that we compare with our RSL to constrain regional effects (Fig. 10); 3) long-term (~century) tide gauge records from six sites maintained by NOAA (Bar Harbor, ME; Portland, ME; Montauk, NY; The Battery, NY; Sandy Hook, NJ; and Atlantic City, NJ; Holgate et al., 2013) along the U.S. East Coast; and 4) a GMSL record covering the last 130 years derived from tide gauge observations (Church & White, 2011).

The structure of the model was centered around generating RSL estimates for the 16 geographical groupings established in the Engelhart & Horton (2012) dataset, which includes a grouping of sea-level index points and constraining data from Southern Massachusetts. The model considers the degree of RSL covariance for each location and accounts for stronger intraregional covariance and weaker interregional covariance. The subdivisions are defined as northeastern Atlantic (inclusive of southern Massachusetts), mid-Atlantic, and southern North Atlantic (following Engelhart & Horton, 2012. The model also reflects RSL covariance with GMSL, which is a component of local and regional RSL variation. Differences between the GMSL curve and RSL changes at given locations are primarily due to vertical land motions, especially Glacial Isostatic Adjustment (e.g., Peltier & Fairbanks, 2006). In updating Engelhart & Horton (2012), we used a considerable amount of RSL data from other locations, as well as the GMSL records. Considering the relatively

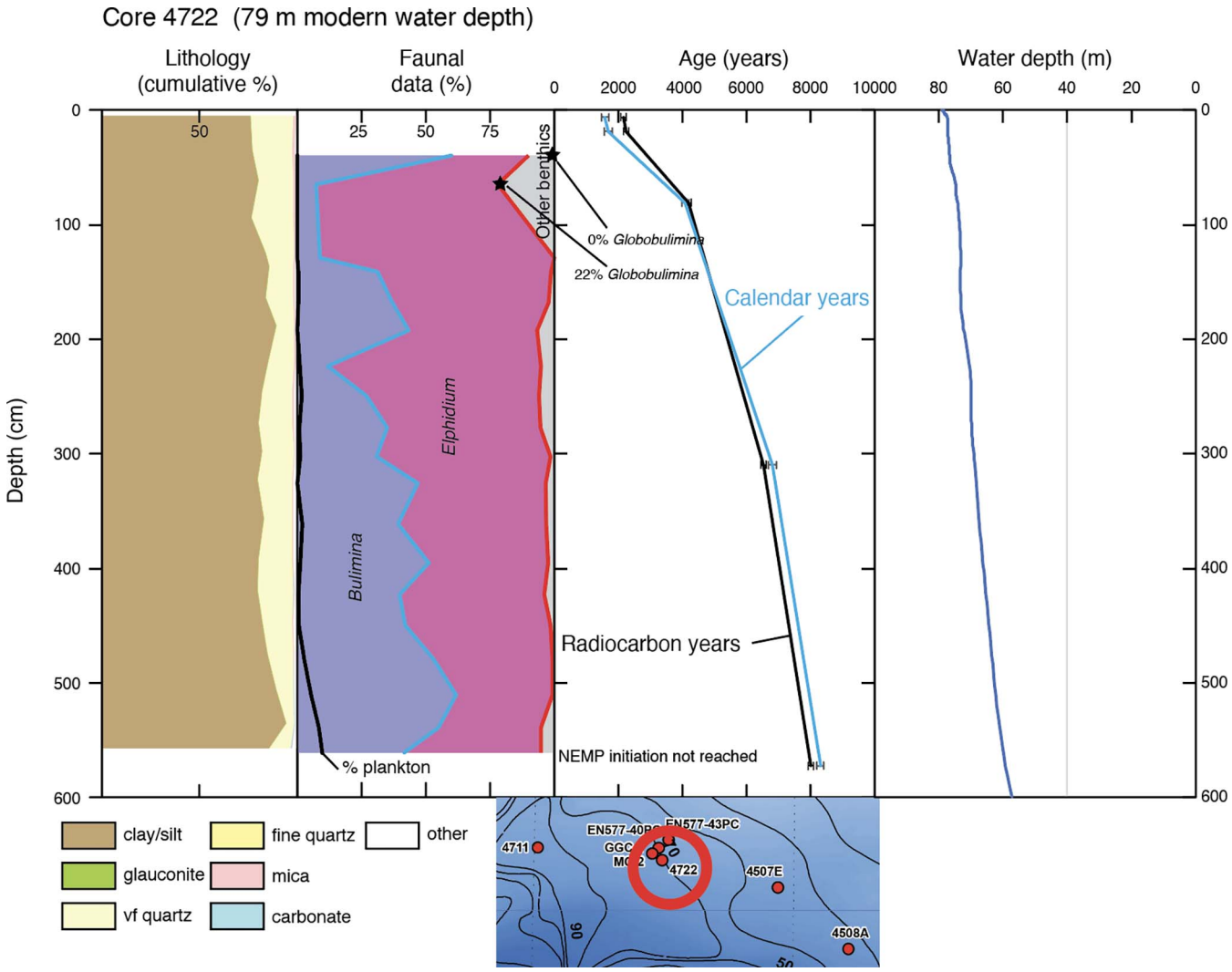

FIGURE 5. Cumulative percentage of lithology, cumulative percentage of benthic foraminiferal biofacies, percent planktonic foraminifera of total foraminifera (black line), and ages (black = radiocarbon years; blue = calendar years) plotted versus depth in Vibracore 4722. Inset map shows core locations with 4722 circled. Legend shows lithologies: vf = very fine sand, f = fine sand, m = medium sand, c-vc = coarse to very coarse sand. Water depth (m) estimates were derived by differencing our southern Massachusetts RSL from current water depth.

sparse database of Holocene RSL samples in any given location along the U.S. East Coast (inclusive of southern Massachusetts), modeling the covariance of data from the entire U.S. East Coast and GMSL records facilitated a more robust estimate of RSL in southern Massachusetts. Ultimately the model produced: 1) an estimate of Holocene RSL variation for southern Massachusetts; 2) the rate of that RSL variation; and 3) uncertainties of the estimates of RSL and RSL rates.

We used the southern Massachusetts RSL record to provide predicted paleodepths for each core through the Holocene. The RSL estimates in age were projected onto core depths (Figs. 3–8) using the calendar age calibration points and the RSL position subtracted from the present depth to give predicted paleowater depths.

RESULTS

CORE 4507

Core 4507 (91 m water depth; Fig. 3) is on the eastern margin of the NEMP (Fig. 1) where the top sample is muddy sand (65% sand). It shows a fining upward pattern from fine-medium quartz sand at its base (older than 10,000 radiocarbon years before present) to 350 cm. This core penetrated into the underlying sand ridges and the shift to mud deposition occurred at about 350 cm with a radiocarbon age of 10,070 yr and calendar age of 11.0 ka (Fig. 1; Table 1). Mud reaches peak concentration (~50%) between 350 and 200 cm (11.0–6.0 ka), and sand increases above this (~65% sand). Benthic foraminifera are dominated by *Bulimina marginata* (typically 50%). The *B. marginata* biofacies is remarkably constant from ~320 cm to 50 cm. *Elphidium* (primarily *E. excavatum* subspecies, though species and subspecies were not rigorously differentiated due to complexity of this group; Miller et al., 1982) becomes subdominant above 175 cm (~5 ka) and the top sample (Common Era, last 2,000 years) is dominated by an *Elphidium-B. marginata* biofacies. A peak in percent planktonic foraminifera occurs at ~300 cm (~9 ka) and decreases at ~250 cm (~8 ka). The plankton are dominated by transitional forms (*Globorotalia inflata*, *Neogloboquadrina dutertrei*) and subpolar forms (*Neogloboquadrina incompta*, *Globigerina bulloides*),

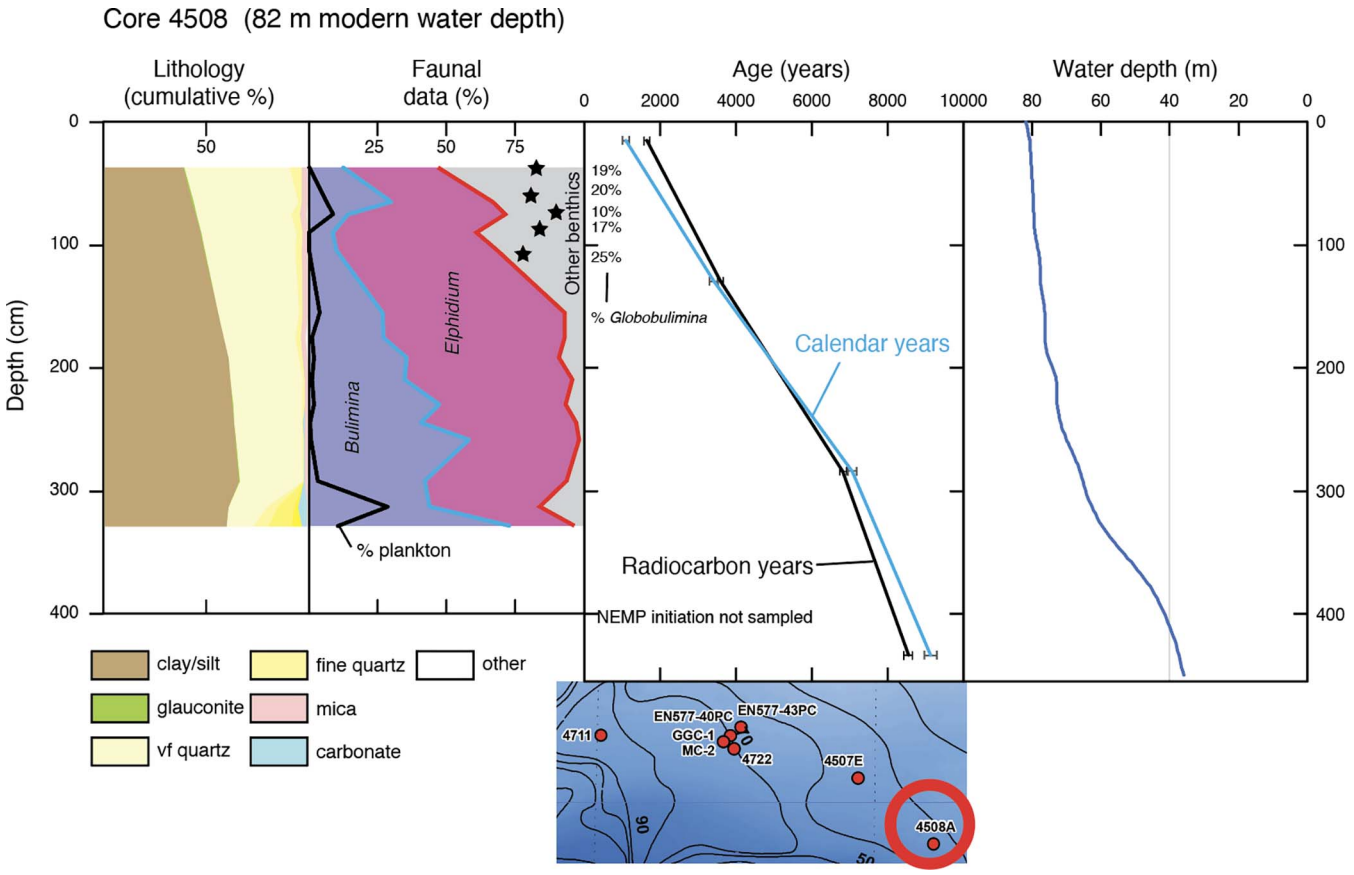

FIGURE 6. Cumulative percentage of lithology, cumulative percentage of benthic foraminiferal biofacies, percent planktonic foraminifera of total foraminifera (black line), and ages (black = radiocarbon years; blue = calendar years) plotted versus depth in Vibracore 4508. Inset map shows core locations with 4508 circled. Legend shows lithologies: vf = very fine sand, f = fine sand, m = medium sand, c-vc = coarse to very coarse sand. Water depth (m) estimates were derived by differencing our southern Massachusetts RSL from current water depth.

but also include thermophilic taxa (*Orbulina universa*, *Globigerinoides ruber*, *G. ruber (pink), G. sacculifera*, and *Globorotalia menardii*), and deep dwelling forms (*Globigerinoides conglobatus*) not normally found in the region, but found in the adjacent Sargasso Sea and in warm core rings derived from it (Bé & Tolderlund, 1971).

CORE 4711

Core 4711 (81 m water depth; Fig. 4) is the westernmost core in the heart of the NEMP as defined by the thickness maps of Bothner et al. (1981; Fig. 1) with only about 5% sand in the top sample. This core contains a thicker sandy section at its base with percent sand decreasing upsection from nearly 100% sand at 450 cm to nearly all mud at 325 cm (Fig. 4). The section from 300 cm to the top is uniform mud (>95%). The sand is older than 9.0 ka (the lowermost radiocarbon date at 317–337 cm is 8,630 yr), but the transition from sand to mud is certainly younger than at core 4507 (ca. 11 ka). This suggests that the development of the main NEMP occurred during the Early Holocene (ca. 9 ka), though mud deposition began earlier in the deeper water (91 m) to the east (ca. 11 ka). Lower Holocene benthic foraminifera (~350–250 cm) are dominated by *B. marginata*, which continue into the Middle Holocene and decrease in abundance above 175 cm (7 ka, Fig. 4). *Elphidium* is subdominant in the Lower Holocene below 175 cm but increases to dominance above 175 cm. In contrast to Core 4507 where *Elphidium* increases in abundance with increasing sand (Fig. 3), the change to the *Elphidium* biofacies is not associated with a change in lithology (Fig. 4). Planktonic foraminifera are common (25–50% of total foraminifera) in the Lower Holocene section (380 cm, ~9 ka) and become rare and dominated by juveniles in the Middle to Upper Holocene above ~325 cm. Planktonic foraminifera are similar to those in core 4507, with common thermophilic species.

CORE 4722

Core 4722 (79 m water depth; Fig. 5) is located on the northeastern part of the main mud lobe centered on core 4711 and near the closely spaced *Endeavor* 577 cores (Chaytor et al., 2022). Core 4722 contains slightly sandy mud throughout its length (550 cm, 8.3 ka), with a faint coarsening upward trend to ~70% mud at the top (Fig. 5). This core does not date the initiation of mud deposition, except to constrain it as older than 8.3 ka. The lower part of the core (below ~320 cm) is co-dominated by *B. marginata* and *Elphidium* (both ~50%; Fig. 5), with the latter becoming dominant above 320 cm. As in Core 4711, the increase in *Elphidium* is not associated with a major increase in sand. Planktonic

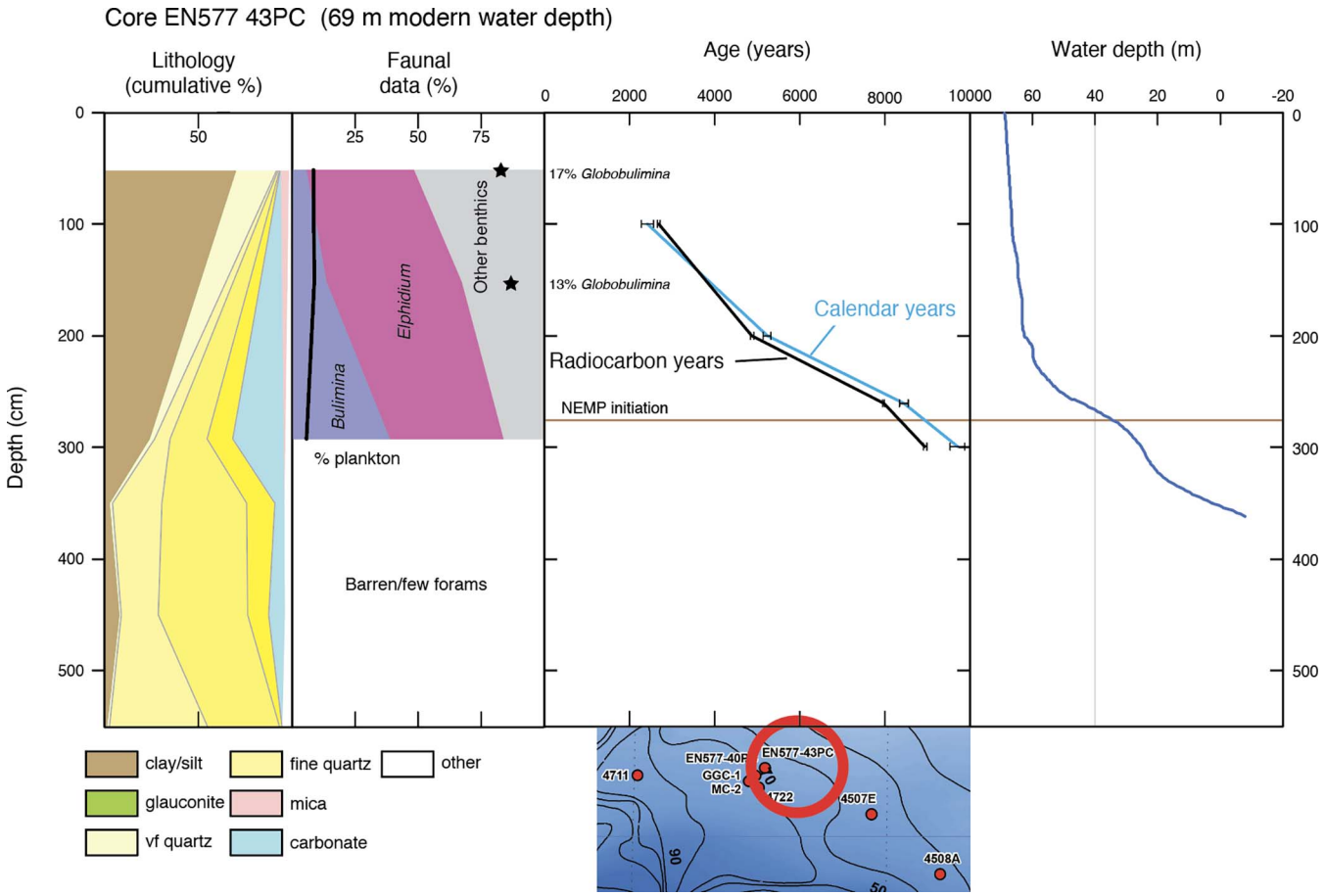

FIGURE 7. Cumulative percentage of lithology, cumulative percentage of benthic foraminiferal biofacies, percent planktonic foraminifera of total foraminifera (black line), and ages (black = radiocarbon years; blue = calendar years) plotted versus depth in piston core EN577-40PC. Inset map shows core locations with EN577-40PC circled. Legend shows lithologies: vf = very fine sand, f = fine sand, m = medium sand, c-vc = coarse to very coarse sand. Water depth (m) estimates were derived by differencing our southern Massachusetts RSL from current water depth.

foraminifers are relatively rare compared to other cores but are most common in the base of the core (~8 ka) and again include rare thermophilic species (e.g., *Orbulina*).

CORE 4508

Core 4508 (82 m water depth; Fig. 1) is located in the eastern NEMP and is dominated by muddy sand (40% mud; Fig. 6) in the top 100 cm. The core shows a distinct coarsening upward succession from a mud peak at 290 cm dated as ~8 ka, with a mean sedimentation rate of 50 cm/kyr between 15 cm and 290 cm (Fig. 6; Bothner et al., 1981). We did not sample below 320 cm, though a radiocarbon data of 9,400 yr (10.0 ka) at 419–440 cm suggests even higher Early Holocene sedimentation rates (Fig. 6; Bothner et al., 1981). This core is dominated by *B. marginata* (~50%) below 220 cm with *Elphidium* spp. increasing up section as in other cores. Planktonic foraminifera are common in the lower part of the core (~8 ka), with a few thermophilic species.

CORE EN577-43PC

This core (69 m water depth) penetrated well into the sands (Unit 3 of Chaytor et al., 2022) that predate the NEMP (Fig. 7). The section fines upward above 300 cm. The timing of the shift to mud deposition began between 9,160 yr and 8,160 radiocarbon yr (9.9 to 8.9 ka calendar), though mud did not become dominant until the top ~150 cm (last 3,000 years). Benthic biofacies are dominated by *B. marginata* and *Elphidium* in the sandy muds, with *Elphidium* and other taxa, including common (13–17%) *Globobulimina* in our samples, increasing upsection as the section shifts to dominant mud (Fig. 7). Planktonic foraminifera are sparse in this core.

CORE EN577 40PC

Core EN577 40PC is located in the northeastern NEMP near core 4722 (Fig. 1) and is dominated by mud above 575 cm (Fig. 8). Below 575 cm, the section coarsens down. A radiocarbon date of 8,300 yr (8.8 ka) at 565 cm dates the initiation of the NEMP at this location (Chaytor et al., 2022). The sample from 600 cm (~9 ka) is dominated by *B. marginata* (64%), with subdominant *Elphidium* (30%). The sandy muds above this are mostly dominated by *Elphidium* with subdominant *B. marginata*, with two notable exceptions. The sample at 575 cm contains a more diverse shelfal assemblage of *Nonionella*, *Pyrgo*, *Lagena*, *Fursenkoina*, and *Lenticulina* associated with the influx of planktonic foraminifera. The sample at 150 cm (~3000 yr) is dominated by *G. affinis*

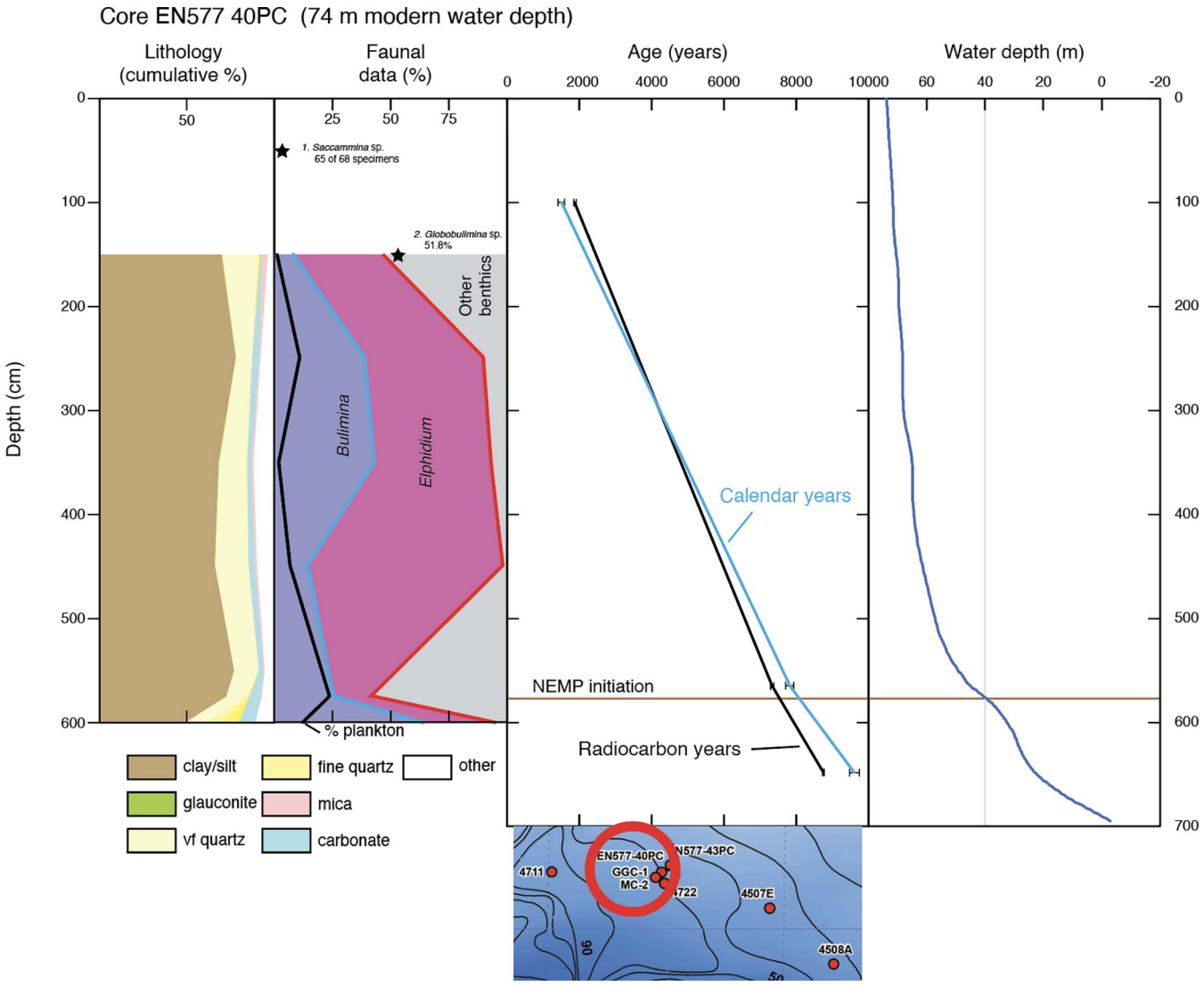

FIGURE 8. Cumulative percentage of lithology, cumulative percentage of benthic foraminiferal biofacies, percent planktonic foraminifera of total foraminifera (black line), and ages (black = radiocarbon years; blue = calendar years) plotted versus depth in piston core EN577 43PC. Inset map shows core locations with EN577-43PC circled. Legend shows lithologies: vf = very fine sand, f = fine sand, m = medium sand, c-vc = coarse to very coarse sand. Water depth (m) estimates were derived by differencing our southern Massachusetts RSL from current water depth.

(51.8% in our sample), which continues upsection (Chaytor et al., 2022). Planktonic foraminifera are rare but more common in the lower part of the core with numerous *Orbulina* present at 449 cm.

OC326 CORE GGC-1

This core was obtained by L. Keigwin for stable isotopic analysis, and we have not evaluated the lithostratigraphy and benthic foraminiferal changes other than the appearance and dominance of *G. affinis* over the top 200 cm (3.2 ka; Fig. 9). Single specimen $\delta^{18}O$ analyses of *G. affinis* ($\delta^{18}O_{benthic}$) over the past 3000 years show a ~1‰ variation for the typically four analyses at each level (Fig. 9). We show the predicted annual $\delta^{18}O_{seawater}$ range for a range ~4–5°C and 0.3–0.4 psu of 0.95‰ (mean 1.45 ± 0.34‰ 1σ) computed using the Levitus temperature and salinity data and the paleotemperature equation (O'Neil et al., 1969; Fig. 9). Thus, the range observed in $\delta^{18}O_{benthic}$ values (Fig. 9) reflects a shelf bottom water annual cycle. This illustrates that single specimen $\delta^{18}O_{benthic}$ measurements reflect annual variability.

DISCUSSION

BENTHIC FORAMINIFERAL BIOFACIES

Our benthic foraminiferal studies show that despite shelf currents focusing mud in this area, deposition is *in situ*, reflecting typical middle to outer shelf biofacies. We can recognize three predominant biofacies in vertical succession: *B. marginata*, *Elphidium-B. marginata*, and *Globobulimina*. The benthic foraminiferal biofacies in the NEMP cores we examined generally show a change from sandier Lower Holocene sediments that were dominated by a *B. marginata* biofacies to Middle Holocene *Elphidium-B. marginata* fauna, with the change dated at ca. 7–6 ka. The modern inner to inner-middle neritic zone in the MAB

TABLE 1. Radiocarbon and calendar ages.

Depth range (cm)	Depth (cm)	C14 age (years)	Radiocarbon age ± error (years)	Cal age Marine20	error	
EN577-43PC						
100	100	2750	30	2293	82	
200	200	5000	40	5128	102	
260	260	8160	30	8476	141.5	
299	299	9160	40	9704	107.5	
EN577-40PC						
100	100	2130	30	1537	79	
565	565	8300	35	8635	94	
648	648	9900	30	10726	103.5	
4507						
0–40	20	1980	80	1381	99.5	
93–123	108	4050	90	3897	144	
150–180	165	5180	60	5352	94.5	
220–250	235	6720	90	7023	124.5	
323–353	338	10070	90	10967	152	
4508						
0–30	15	1820	80	1212	99	
113–143	128	3940	80	3751	127.5	
271–293	281	7500	100	7778	116.5	
419–440	429.5	9400	120	10040	177.5	
4711						
0–6	3	2020	80	1422	101	
18–22	18.5	2340	60	1786	98.5	
70–90	80	5470	70	5656	103	
200–230	215	7630	110	7907	131	
317–337	327	8630	100	9091	148	
4722						
0–12	6	2170	80	1585	114	
16–21	18.5	2250	90	1678	126	
69–93	81	4200	70	4096	123.5	
300–320	310	6540	90	6818	129	
568–588	573	8010	90	8301	111.5	
OCE326 GGC-1 + trigger core						Fm
1.5	1.5			>Modern		1.0005
14	14			605	15	0.9276
16	16			690	25	0.9177
18	18			630	15	0.9245
23	23			720	20	0.9142
34	34			720	20	0.9143
40	40			790	20	0.9066
45	45			715	20	0.9146
50	50			1350	35	0.84501
200	200			3160	40	0.67472

(<45 m) is dominated by *Elphidium* spp. (Poag et al., 1980), though in the NEMP *Elphidium* begins to dominate at the paleodepth of ~60–75 m (water depths obtained correcting for RSL; Figs. 3–8). There is no evidence of downslope transport including shallow-water taxa, and we interpret the *Elphidium* as *in situ* and dominating the fauna due to stressful conditions of very high sedimentation rates. During the Late Holocene, *Globobulimina* increased in abundance (last 3,000 years), though this is not reflected in many samples likely due to post-coring dissolution.

Mud Patch Initiation

Our examination of cores from across the NEMP allow us to better constrain the timing of the development of the mud patch. Mud deposition began in the NEMP during the Early Holocene (9–11 ka; Fig. 11) and shows that development of the mud deposition was diachronous as a function of water depth. In the cores we examined, two indicate initiation at ca. 9 ka (4711, EN577-40PC; Figs. 4, 8) and two are consistent with that timing (4722, 4508; Figs. 5. 6, 11). However, core 4507 (91 m water depth) indicates an earlier age of initiation (ca. 11 ka; Figs. 3, 11). Radiocarbon dates on numerous cores examined by Chaytor et al. (2022) on the eastern part of the main mud patch lobe (Fig. 1) constrain the timing of mud initiation in that area. As noted, their cores EN577-40PN and EN577-43PC suggest a 9-ka initiation (Figs. 6, 7). EN577-9PC (not shown) has a date of 9.5 ka on Unit 2, the transitional unit from sands to muds; EN577-4PC has a date that suggests an older initiation of mud deposition with a date of 9.9 ka; and core EN-577-53PC has a date of 10.4 ka. Thus, the initiation of mud deposition spanned 2 kyr (11–9 ka; Fig. 11). Chaytor et al. (2022) hypothesized that erosion of the ridge tops during sea-level rise might have resulted in a slightly older age for the top sand base mud at this location. However, examining the initiation of mud deposition as a function of water depth (Figs. 3–8) shows that oldest mud deposition was initiated in water depths of 40 ± 10 m (i.e., applying the RSL record Fig. 10 to the present water depths; Figs. 3–8). This suggests that mud deposition began when locations reached positions below mean storm wave base (~30–50m; Grant, 2019).

Benthic Foraminiferal Biofacies and Sea-level Rise

The RSL rise on the Massachusetts shelf (Fig. 10) has been constrained by index and limiting points in previous studies (Fig. 10; Engelhart & Horton, 2012; Horton et al., 2013). Our Gaussian process analysis provides a record of RSL and rates of rise that show the Glacial Isostatic Adjustment (GIA) component of RSL, as illustrated by the difference between GMSL and RSL (Fig. 10). We note the predicted response of GIA subsidence (e.g., Peltier, 2004) and illustrated by Engelhart & Horton (2012: 1) GIA-induced subsidence over the past 9 kyr (i.e., with RSL lower than GMSL; Fig. 10); and 2) minimal to no GMSL rise during the Common Era with GIA as the dominant but decreasing contribution to RSL at that time. Our sea-level records (Fig. 10) provide a template for understanding the relationship of mud deposition to sea level and of benthic foraminiferal fauna to water depth changes.

Early Holocene RSL rose from 45 to 20 m below present from ca. 11.7 to 8 ka at a rate that decreased from greater than 10 to approximately 7 mm/yr (Figs. 10, 11). The mud patch was preceded (>11 ka; sea levels 45 m shallower than the present 70–91 m) by shelly inner neritic sand with sand dollars (*Dendraster excentricus*) and sea scallops (*Pecten*) noted in the cores (Chaytor et al., 2022; Keigwin, personal observation) that are consistent with an inner neritic interpretation for these sands (i.e., less than 40 m; Merrill & Hobson, 1970). The *B. marginata* biofacies became established during the Early Holocene (>8.2 ka) when paleowater depths reached 40–60 m (Figs. 3–8). The *B. marginata* biofacies first occurs in sands and continues into the muds, indicating little substrate control. The development of the *B. marginata* biofacies in sandy sediments is constrained at core 4711 (81 m present depth) as older than 9.0 ka (Fig. 4), though its dominance is primarily an early Middle Holocene widespread event in the nascent mud patch (ca. 9–7 Ma).

Relative sea level slowed during the early Middle Holocene and rose from 20 m below present to 5 m below present from 8.1–5 ka, as the rate of rise slowed from ~7 to 2 mm/yr. It was

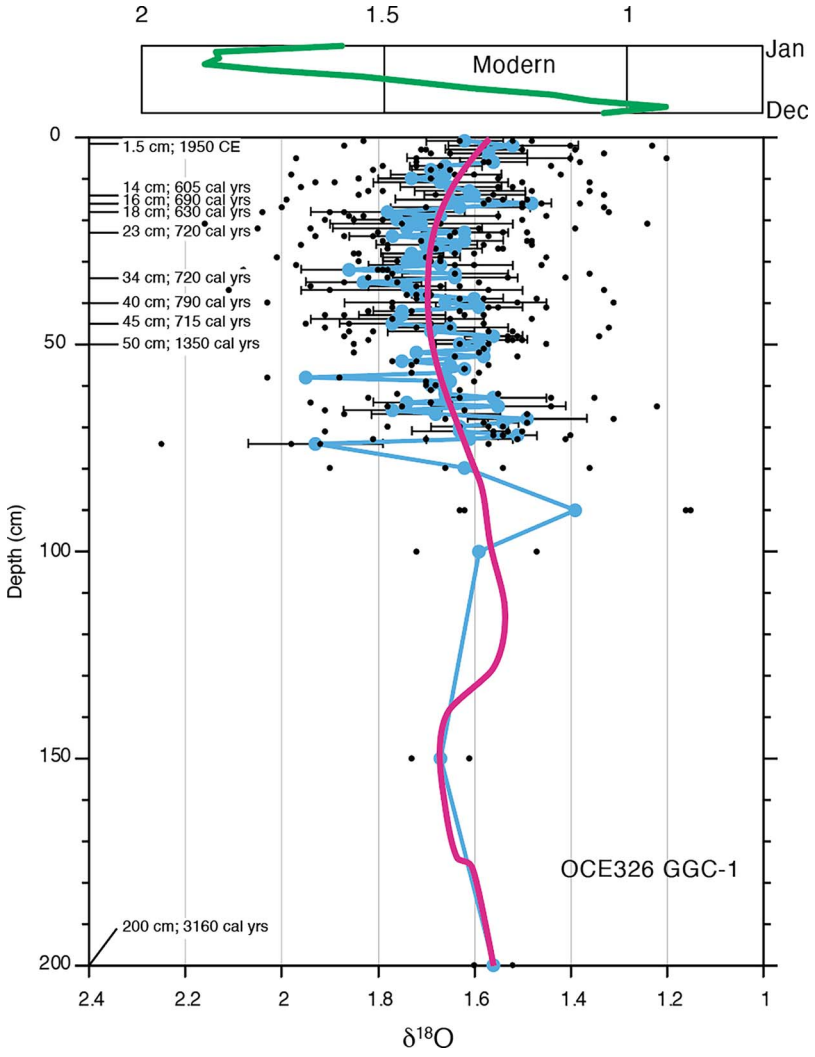

FIGURE 9. Single specimen $\delta^{18}O$ measurements of *Globobulimina affinis* from core OCE326 GGC-1 versus core depth in cm showing calibrated radiocarbon ages in calendar (cal) years. Average with 1s error at each level is show in light blue. Blue line is a running mean and magenta line is a LOESS (locally estimated scatterplot smoothing) fit. Green line is plotted versus month of year and shows the mean annual predicted $\delta^{18}O$ values by month. Note that the measured single specimen $\delta^{18}O$ data faithfully replicate the predicted annual range.

during this period of slowly rising sea level with widespread mud deposition that *Elphidium* spp. joined *B. marginata* as co-dominant. It is somewhat counterintuitive that the shallow *Elphidium* biofacies that generally typifies the inner-middle neritic zone (<45 m; Poag et al., 1980) developed in water depths that were greater than the supposedly deeper water *B. marginata* biofacies. However, the total amount of sea-level rise was small after mud deposition began (Figs. 3–8). The *Globobulimina* biofacies developed in near-modern water depths during the most widespread developments of the mud patch over the past 3,000 years as sea level slowed to 1 mm/yr. Our analysis, which includes historical tide gauge data, show an acceleration of rise in the past 100 years.

We find that as RSL rose and slowed, mud deposition began when the cores (current depths 69 to 91 m) reached paleodepths of 40 to 60 m (Fig. 11). Mud deposition began in the deepest core (4507; 91 m) at ca. 11 ka when it was at ~40 m and later (ca. 9 ka) at the shallower cores. This suggests a minimal depth of 40 ± 10 m below storm wave base for the initiation of mud deposition. Benthic foraminifera and age dates (Figs. 3–8) provide constraints on what makes the NEMP unique versus other locations in the mid-Atlantic Bight that are currently dominated by sand sheet and ridge deposition. The development of the mud patch was associated with very high sedimentation rates (30–79 cm/kyr) and an opportunistic *Elphidium-B. marginata* fauna. The high sediment accumulation rates suggest that the mud patch was formed as mud was focused by shelf currents in a region with minimal velocities (Roarty et al., 2019) on this portion of the continental shelf when it fell below storm wave base.

CONTROLS ON BENTHIC FORAMINIFERAL BIOFACIES

Our benthic foraminiferal studies allow us to address controls on benthic foraminiferal distributions on the shelf and slope. The benthic foraminiferal biofacies are not directly indicative of water depth, oxygen, or substrate (mud versus sand), though they do display vertical variations that reflect the evolution of the NEMP. There is no benthic foraminiferal ecotone (i.e., mixing or transitional changes between distinct biofacies) developed between the Massachusetts continental shelf and slope, such as occurs on the mud-dominated Amazon shelf and slope (Vilela, 1995), though

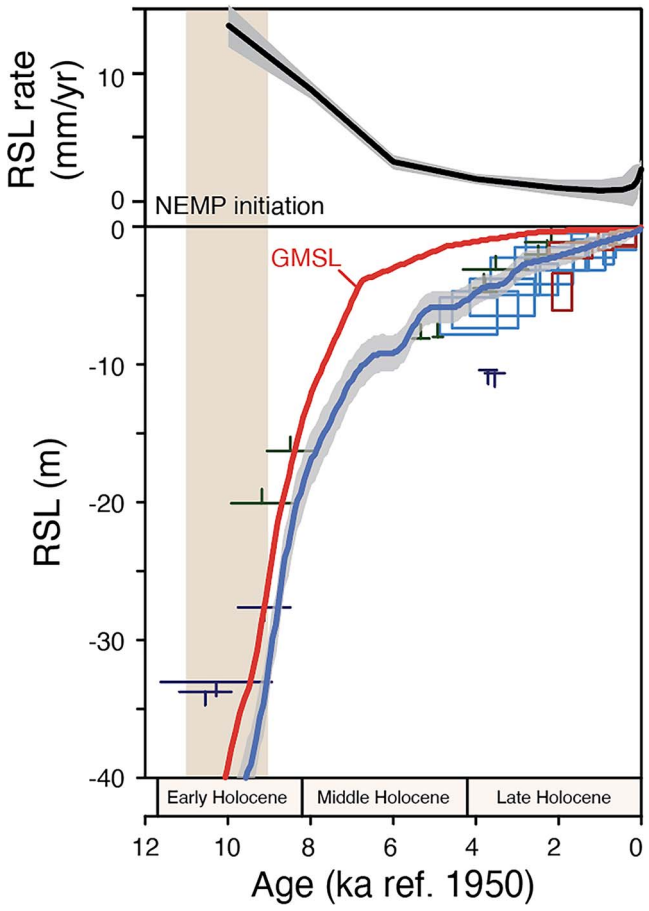

FIGURE 10. Holocene southern Massachusetts relative sea-level rise (RSL; data after Engelhart & Horton, 2012). T = marine limited data, inverted T = terrestrial limited data, boxes are index points (Horton et al., 2013). Blue line is a Gaussian model from this study showing best fit and rates of sea-level change for Holocene southern Massachusetts relative sea-level rise with 1 sigma errors in gray. Red line is GMSL estimate of Lambeck et al. (2014). NEMP initiation shown as tan shaded interval from 11.0 to 9.0 ka.

we note that the high abundances of *Globobulimina* transcend the shelf-slope break. *Globobulimina* is found in abundance in the oxygen minimum zone on the slope south of the NEMP (Miller & Lohmann, 1982) and in the past 3,000 yr in the NEMP. Low oxygen in pore waters favors *Globobulimina*, which is one of the few eukaryotes that thrive in anoxic conditions. As noted, anoxia is not realized either on the NEMP over the last 3,000 years or in the modern oxygen minimum zone on the slope, though in the oxygen minimum zone O_2 concentrations begin to be limiting for sensitive taxa (3 mL/L; 134 mmol/L). Our results are consistent with the premise that *Globobulimina* is a low-oxygen taxon.

Uvigerina is a benthic foraminifera that has been also used as a low-oxygen water mass indicator (e.g., Streeter, 1973), though on the Massachusetts continenal slope it reaches peak abundance well below the oxygen minimum zone and is associated with high silt and TOC (Miller & Lohmann, 1982). We thought comparisons between organic-poor and moderately organic-rich cores might show higher abundances of *Uvigerina* in the latter. We do see higher abundances of *Uvigerina* in core 4508 with higher TOC, though the peak abundance is only 3%, and *Uvigerina* is lacking in many samples. The relative scarcity of *Uvigerina* in the NEMP is interesting because on ancient (Miocene-Eocene) shelves in this region, *Uvigerina* dominated the deeper middle neritic zone (>75 m) biofacies (e.g., Browning et al., 2006). The lower-than-expected abundance of *Uvigerina* is likely a result of the very high accumulation rates (30–79 cm/kyr) of sediments that apparently favor *Globobulimina* (in areas of low oxygen in the sediments) and *Elphidium* (an opportunistic genus), and perhaps *B. marginata*. *Uvigerina* is present but does not dominate in percentage data, reflecting the closed sum problem in percent data and the greater mass accumulation rates of the dominant taxa.

While benthic foraminiferal biofacies from the NEMP are generally consistent with previous biofacies studies of the MAB continental shelf (Buzas & Culver, 1980; Culver & Buzas, 1980; Gevirtz et al., 1971; Murray, 1973; Parker, 1948; Poag et al., 1980), there are important differences. We do not see the *Saccammina* (northern MAB; other than samples impacted by post-coring dissolution, see below) or *Cibicidoides* (southern MAB) biofacies reported by Poag et al. (1980) from sandy shelf sediments except in one dissolved sample (see below). Rather we see an ecotone of their inner shelf *Elphidium* and their outer shelf *B. marginata* biofacies. The biofacies are unique as is their depositional setting, the NEMP.

The development of the mud patch was associated with an *Elphidium-B. marginata* fauna (Fig. 11). We suggest that this fauna was favored by the very high sedimentation rates of the developing mud patch. As RSL rise decreased dramatically in the last 3,000 years, anoxia developed at least seasonally in the upper sediments likely due to increased organic matter (e.g., Cores 4711 and 4722; Figs. 4, 5). There is some relationship of benthic biofacies to water depth, with the *B. marginata* biofacies developing only when waters depths exceeded 40–50 m (Figs. 3–8).

Early Holocene Peak in Planktonic Foraminifera

An Early to early Middle Holocene peak in percent planktonic foraminifera is associated with warm-water taxa. It has long been known that the percent planktonic foraminifera of total foraminifers in shelf-slope sediments increases with water depth across the continental shelf and slope (Grimsdale & van Morkhoven, 1955), and the percentage of planktonic foraminifers has been calibrated statistically to water depth (van der Zwaan et al., 1990). However, this metric is imperfect because the percent planktonic foraminifera is also related to dissolution, productivity, and oceanographic effects (Berger & Diester-Haass, 1988). On the NEMP, oceanographic effects control the abundance of planktonic foraminifera. In this setting, we suggest that the increase in percent planktonic foraminifera and the associated invasion of warm taxa was from incursions of warm core rings. We speculate that increased tidal energy due to sea-level rise at ca. 8 to 10 ka that has been modeled for this region (Horton et al., 2013) resulted in greater influence of warm core rings on the shelf; however, we cannot rule out that the Gulf Stream was closer to the NEMP in the Early Holocene or that ring production has changed through time (Forsyth et al., 2022).

Globobulimina and Foraminiferal Preservation in Archived Cores

The dominance of *Globobulimina* noted in the >250-μm size fraction over the past 3 kyr (Chaytor et al., 2022) provides

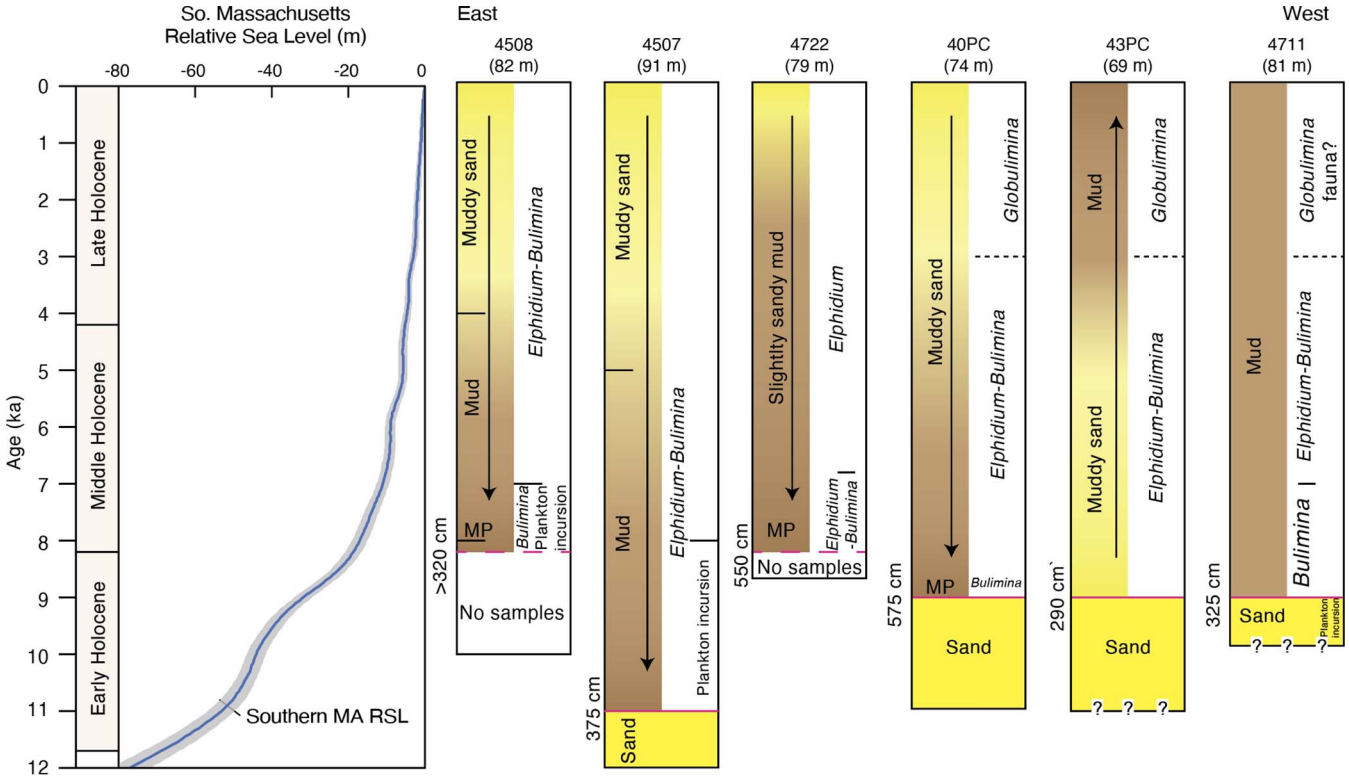

FIGURE 11. History of sedimentation of the NEMP based on the cores examined here. Time scale is GTS2020 (Gradstein et al., 2020). Southern Massachusetts Relative Sea Level is after Fig. 10. Brown = mud, light yellow = sandy mud, dark yellow = sand. Red lines = timing of the development of the mud patch; dashed red lines are uncertain; MP = mud peak. Arrows point in fining direction. The absence of dominant *Globobulimina* in Cores 4508, 4507, and 4722 is likely due to post-coring dissolution.

information on depositional environments and post-depositional preservation. Our samples generally do not reflect these high abundances of *Globobulimina* in part due to the size fraction studies (>150 µm here versus >250 µm in Chaytor et al., 2022) and post coring dissolution (see below), though *Globobulimina* dominated the last 3 kyr on the NEMP in recently obtained cores (Chaytor et al., 2022; Fig. 9). *Globobulimina* is generally considered to be a deep infaunal taxon tolerant of dysoxic and even anoxic conditions (Van der Zwaan et al., 1999). Indeed, this is one of the sole benthic taxa found within Mediterranean sapropels (organic rich beds) that were associated with bottom water anoxia (Katz & Thunell, 1984). It has been a puzzle understanding how benthic foraminifera survive and reproduce in anoxic environments. However, recent studies have shown that foraminifera are the only known eukaryote capable of withstanding anoxic conditions and that *Globobulimina* specifically contains enzymes for nitrate reduction, specifically nitrite reductase and nitric oxide reductase (Woehle et al., 2018). The mud patch is not generally anoxic, for TOC contents are generally moderate (0.5–1.9%; Bothner et al., 1981; Chaytor, personal observation) and generally never reach sapropel levels (>2%). In addition, the continued presence of the *B. marginata-Elphidium* biofacies to the uppermost samples indicates that the sediment-water interface and shallow infaunal environment remained oxic. Nevertheless, the development of the *Globobulimina* biofacies in the last 3,000 years suggests that the deep infaunal environment (e.g., about 10 cm depth) was likely anoxic. Stable sea levels continued moderate mud supply, and moderate to abundant TOC favored the development of the *Globobulimina* biofacies.

The high abundances of *Globobulimina* reported by Chaytor et al. (2022) from the >250-µm size fraction of the EN577 cores and by Keigwin from core OC326 Core GGC-1 (Fig. 10) are less obvious in older Vibracores taken in 1979 (Fig. 3–8). Though present in the top of the first generation Vibracores (e.g., in sample 4711, 0–2.5 cm it comprises 22% of a sparse fauna in the >150-µm size), *Globobulimina* is not as abundant as reported in more recently obtained NEMP cores (Chaytor et al., 2022). *Globobulimina affinis* is an extremely thin-walled taxon that is readily dissolved, particularly in the region of moderate TOC. We suggest that this is due to post-coring dissolution. Post-depositional fluids must have been sufficiently acidic and dissolved the more fragile taxa. Caution must be exercised in sampling older cores (in this case 30+ years after coring), recognizing that in some settings, post-coring dissolution will remove foraminiferal taxa.

We also observe that preservation of thin-walled taxa such as *Globobulimina* can be ephemeral. We resampled Core EN577 40-PC at 50–52 cm in 2023 and found no *Globobulimina* in the >150 µm size fraction, though this taxon was dominant in samples taken in this interval in 2017 (Chaytor et al., 2022). Rather, we found only 68 specimens dominated by the agglutinated form *Lagenammina difflugiformis* with rare *Elphidium* and *B. marginata*. This strongly suggests that dissolution occurs in these organic-rich sediments soon after coring.

Temperature Changes and $\delta^{18}O$

We show that single specimen measurements reflect annual variability (Fig. 9), which implies fairly short (weeks to a few months) lifespans for *G. affinis*. The Late Holocene $\delta^{18}O_{benthic}$ data show relative stability in annual temperatures over the top 200 cm (~last 3 kyr). Variability in $\delta^{18}O_{benthic}$ increases from 30–40 cm, with generally higher $\delta^{18}O_{benthic}$ values that reflect colder and/or more saline bottom waters; this interval includes the Little Ice Age. Above about 15 cm (younger than ~300 years), $\delta^{18}O_{benthic}$ values are lower (warmer and/or fresher). This warming may reflect recovery from the Little Ice Age and anthropogenic warming, though this transition, if real, is not dateable using ^{14}C due to uncertainties in the marine reservoir effect.

CONCLUSIONS

The mud patch south of Cape Cod and Martha's Vineyard, Massachusetts, is a unique feature of the mid-Atlantic Bight continental shelf in that it contains rapidly deposited (>30 cm/kyr) Holocene sandy muds and muddy sands that are graded in profiles across the shelf. The NEMP is the only open-water shelf location in the western North Atlantic (as opposed to shelf basins as in Gulf of Maine or Emerald Basin) that provides high-resolution records of the Holocene. The lithofacies and biofacies work presented here forms a basis for developing such paleorecords of climate and upper ocean (mixed layer) circulation. Benthic foraminifera indicate largely *in situ* conditions in cores we examined. The mud patch developed in the late Early Holocene (ca. 11–9 ka) and was fully developed by ca. 8 ka as water depth reached 40 ± 10 m, and sea-level rise slowed from approximately >10 mm/yr to 2 mm/yr (8–5 ka) and ultimately 1 mm/yr (5–0 ka). A pioneering *B. marginata* biofacies was established in sands prior to mud deposition in paleodepths of 40–60 m and persisted during the establishment of the mud patch. Planktonic foraminifera may have invaded the shelf via warm core rings during the Early Holocene. *Elphidium* increased in abundance in the Middle Holocene (8.1–4 ka) middle neritic zone and continued into the Late Holocene (4.1–present), with a dominance by a *B. marginata-Elphidium* biofacies in sandy muds to muddy sands. We interpret these as opportunistic taxa dominating due to very high sedimentation rates. *Globobulimina* increased in abundance during the Late Holocene (last 3,000 years) favored by stable sea levels, continued moderate mud supply, and moderate to abundant organic carbon. However, older cores only capture some of this increase in *Globobulimina* abundances due to probable post-coring dissolution. Analyses of single specimens of *Globobulimina* over the past 3,000 years capture the annual range in $\delta^{18}O_{seawater}$ of 0.95‰ associated with annual temperature changes of ~4–5°C and 0.3–0.4 psu and seem to record a temperature minimum associated with the Little Ice Age and subsequent natural and anthropogenic warming.

ACKNOWLEDGMENTS

This paper is dedicated to the memory of Martin A. Buzas, a pioneer in benthic foraminifera on the U.S. Atlantic margin, whose contributions on this topic range from an early paper on Long Island Sound foraminifera to a classic synthesis of distributional data on Holocene benthic foraminifera of the North American Atlantic continental margin. His loss prompted us to rejuvenate this study of the intriguing deposits of the mud patch. We thank J. Broda (WHOI) for access, E. Roosen (WHOI), and B. Buczkowski (USGS) for core photographs and sampling, W. Si for sampling, E. Franks for stable isotope analyses, R. Mortlock for conversion of radiocarbon dates, and M. K. Bartlett, K. B. Jones, and two anonymous reviewers for reviews. This study was initiated in 2014 as part of an undergraduate Aresty summer internship by M. Richtmeyer. We thank A. R. Bottge for picking support and J. W. Wright for discussions of oxygen isotopes. Any use of trade, firm, or product names is for descriptive purposes only and does not imply endorsement by the U.S. Government.

REFERENCES

Ashe, E. L., Cahill, N., Hay, C., Khan, N. S., Kemp, A., Engelhart, S. E., Horton, B. P., Parnell, A. C., and Kopp, R. E., 2019, Statistical modeling of rates and trends in Holocene relative sea level: Quaternary Science Reviews, v. 204, p. 58–77.

Bandy, O. L., and Arnal, R. E., 1960, Concepts of Foraminiferal Paleoecology: American Association of Petroleum Geologists Bulletin, v. 44, p. 1921–1932.

Barker, R. W., 1960, Taxonomic notes on the species figured by H.B. Brady in his report of the foraminifera dredged by HMS Challenger during the years 1873-1876: SEPM Special Publication, v. 9, p. 1–238.

Bé, A. W., and Tolderlund, D. S., 1971, Distribution and ecology of living planktonic foraminifera in surface waters of the Atlantic and Indian Oceans, *in* Funnell, B. M., et al. (eds.), The Micropalaeontology of Oceans: Cambridge University Press, Cambridge, p. 105–149.

Beardsley, R. C., and Boicourt, W., 1981, On estuarine and continental-shelf circulation in the Middle Atlantic Bight., *in* Warren, B. A., and Wunsch, C. (eds.), Evolution of Physical Oceanography: Scientific Surveys in Honor of Henry Stommel, Volume 1: MIT Press, Cambridge, MA, p. 198–233.

Berger, W. H., and Diester-Haass, L., 1988, Paleoproductivity: The benthic/planktonic ratio in foraminifera as a productivity index: Marine Geology, v. 81, p. 15–25.

Boggess, A. A., Buczkowski, B. J., and Chaytor, J. D., 2021, Sedimentological and geotechnical analyses of marine sediment cores from the New England Mud Patch, U.S. Geological Survey data release. DOI: 10.5066/P9ZYK3PX.

Bothner, M. H., Spiker, E. C., Johnson, P. P., Rendigs, R. R., and Aruscavage, P. J., 1981, Geochemical evidence for modern sediment accumulation on the continental shelf off southern New England: Journal of Sedimentary Research, v. 51, p. 281–292.

Bremer, M. L., and Lohmann, G. P., 1982, Evidence for primary control of the distribution of certain Atlantic Ocean benthonic foraminifera by degree of carbonate saturation: Deep Sea Research Part A: Oceanographic Research Papers, v. 29, p. 987–998.

Browning, J. V., Miller, K. G., McLaughlin, P. P., Kominz, M. A., Sugarman, P. J., Monteverde, D., Feigenson, M. D., and Hernández, J. C., 2006, Quantification of the effects of eustasy, subsidence, and sediment supply on Miocene sequences, mid-Atlantic margin of the United States: Geological Society of America Bulletin, v. 118, p. 567–588.

Bumpus, D. F., 1973, A description of the circulation on the continental shelf of the east coast of the United States: Progress in Oceanography, v. 6, p. 111–157.

Buzas, M. A., and Culver, S. J., 1980, Foraminifera: Distribution of provinces in the western North Atlantic: Science, v. 209, p. 687–689.

Chaytor, J. D., Ballard, M. S., Buczkowski, B. J., Goff, J. A., Lee, K. M., Reed, A. H., and Boggess, A. A., 2022, Measurements of Geologic Characteristics and Geophysical Properties of Sediments From the New England Mud Patch: IEEE Journal of Oceanic Engineering, v. 47, p. 503–530.

Church, J. A., and White, N. J., 2011, Sea-level rise from the late 19th to the early 21st century: Surveys in Geophysics, v. 32, p. 585–602.

Culver, S. J., and Buzas, M. A., 1980, Distribution of Recent benthic foraminifera off the North American Atlantic coast: Smithsonian Contributions to the Marine Sciences, v. 6, p. 1–512.

Culver, S. J., and Snedden, J. W., 1996, Foraminiferal implications for the formation of New Jersey shelf sand ridges: PALAIOS, v. 11, p. 161–175.

Cushman, J. A., 1918, The Foraminifera of the Atlantic Ocean: U.S. National Museum Bulletin, v. 104, p. Parts 1–8.

Emery, K. O., 1968, Relict sediments on continental shelves of world: American Association of Petroleum Geologists Bulletin, v. 52, p. 445–464.

Engelhart, S. E., and Horton, B. P., 2012, Holocene sea level database for the Atlantic coast of the United States: Quaternary Science Reviews, v. 54, p. 12–25.

Forsyth, J., Gawarkiewicz, G., and Andres, M., 2022, The impact of warm core rings on Middle Atlantic Bight shelf temperature and shelf break velocity: Journal of Geophysical Research: Oceans, v. 127. DOI: 10.1029/2021JC017759.

Gevirtz, J. L., Park, R. A., and Friedman, G. M., 1971, Paraecology of benthonic foraminifera and associated micro-organisms of the continental shelf off Long Island, New York: Journal of Paleontology, v. 45, p. 153–177.

Glenn, S., Arnone, R., Bergmann, T., Bissett, W. P., Crowley, M., Cullen, J., Gryzmski, J., Haidvogel, D., Kohut, J., Moline, M., Oliver, M., Orrico, C., Sherrell, R., Song, T., Weidemann, A., Chant, R., and Schofield, O., 2004, Biogeochemical impact of summertime coastal upwelling on the New Jersey Shelf: Journal of Geophysical Research: Oceans, v. 109. DOI: 10.1029/2003JC002265.

Glenn, S., Schofield, O., Chant, R., Kohut, J., Roarty, H., Bosch, J., Bowers, L., Gong, D., and Kerfoot, J., 2007, Wind-driven response of the Hudson River plume and its effect on dissolved oxygen concentration: Environmental Research, Engineering and Management, v. 1, p. 14–18.

Goff, J. A., Reed, A. H., Gawarkiewicz, G., Wilson, P. S., and Knobles, D. P., 2019, Stratigraphic analysis of a sediment pond within the New England Mud Patch: New constraints from high-resolution chirp acoustic reflection data: Marine Geology, v. 412, p. 81–94.

Gooday, A. J., 1988, A response by benthic Foraminifera to the deposition of phytodetritus in the deep sea: Nature, v. 332, p. 70–73.

Gradstein, F.M., Ogg, J.G., Schmitz, M.D., and Ogg, G.M., 2020, Geologic Time Scale 2020, Cambridge MA, Elsevier.

Grant, G., 2019, Pliocene glacial-interglacial sea-level change, Ph.D. thesis: University of Wellington, 207 p.

Grimsdale, T. F., and van Morkhoven, F. P. C. M., 1955, The ratio between pelagic and benthonic foraminifera as a means of estimating depth of deposition of sedimentary rocks, 4th World Petroleum Congress, 473–491 p.

Heaton, T. J., Köhler, P., Butzin, M., Bard, E., Reimer, R. W., Austin, W. E. N., Bronk Ramsey, C., Grootes, P. M., Hughen, K. A., Kromer, B., Reimer, P. J., Adkins, J., Burke, A., Cook, M. S., Olsen, J., and Skinner, L. C., 2020, Marine20—The marine radiocarbon age calibration curve (0–55,000 cal BP): Radiocarbon, v. 62, p. 779–820.

Holgate, S. J., Matthews, A., Woodworth, P. L., Rickards, L. J., Tamisiea, M. E., Bradshaw, E., Foden, P. R., Gordon, K. M., Jevrejeva, S., and Pugh, J., 2013, New data systems and products at the permanent service for mean sea level: Journal of Coastal Research, v. 29, p. 493–504.

Hollister, C. D., 1973, Atlantic continental shelf and slope of the United States—Texture of surface sediments from New Jersey to southern Florida: U.S. Geological Survey Professional Paper, No. 529-M. DOI: 10.3133/pp529M.

Horton, B. P., Engelhart, S. E., Hill, D. F., Kemp, A. C., Nikitina, D., Miller, K. G., and Peltier, W. R., 2013, Influence of tidal-range change and sediment compaction on Holocene relative sea-level change in New Jersey, USA: Journal of Quaternary Science, v. 28, p. 403–411.

Katz, M. E., Browning, J. V., Miller, K. G., Monteverde, D. H., Mountain, G. S., and Williams, R. H., 2013, Paleobathymetry and sequence stratigraphic interpretations from benthic foraminifera: Insights on New Jersey shelf architecture, IODP Expedition 313: Geosphere, v. 9, p. 1488–1513.

Katz, M. E., and Thunell, R. C., 1984, Benthic foraminiferal biofacies associated with middle Miocene to early Pliocene oxygen-deficient conditions in the eastern Mediterranean: Journal of Foraminiferal Research, v. 14, p. 187–202.

Keigwin, L. D., 2004, Radiocarbon and stable isotope constraints on Last Glacial Maximum and Younger Dryas ventilation in the western North Atlantic: Paleoceanography and Paleoclimatology, v. 19. DOI: 10.1029/2004PA001029.

Lambeck, K., Rouby, H., Purcell, A., Sun, Y., and Sambridge, M., 2014, Sea level and global ice volumes from the Last Glacial Maximum to the Holocene: PNAS, v. 111, p. 15296–15303.

Mazzullo, J., Leschak, P., and Prusak, D., 1988, Sources and distribution of late Quaternary silt in the surficial sediment of the northeastern continental shelf of the United States: Marine Geology, v. 78, p. 241–254.

Merrill, R. J., and Hobson, E. S., 1970, Field observations of *Dendraster excentricus*, a sand dollar of western North America: The American Midland Naturalist, v. 83, p. 595–624.

Miller, A.A.L., Scott, D.B., and Medioli, F.S., 1982, *Elphidium excavatum* (Terquem); ecophenotypic versus subspecific variation: Journal of Foraminiferal Research, v. 12, p. 116–144.

Miller, K. G., and Lohmann, G. P., 1982, Environmental distribution of Recent benthic foraminifera on the northeast United States continental slope: GSA Bulletin, v. 93, p. 200–206.

Miller, K. G., Browning, J. V., Mountain, G. S., Sheridan, R. E., Sugarman, P. J., Glenn, S., and Christensen, B. A., 2014, Chapter 3: History of continental shelf and slope sedimentation on the US middle Atlantic margin: Geological Society, London, Memoirs, v. 41, p. 21–34.

Murray, J., 1973, Distribution and Ecology of Living Benthic Foraminiferids: Heinemann Educational Books, London, 397 p.

Natland, M. L., 1933, The temperature and depth-distribution of some recent and fossil Foraminifera in the southern California region: Bulletin of the Scripps Institution of Oceanography: Technical series, v. 3, p. 225–230.

O'Neil, J. R., Clayton, R. N., and Mayeda, T. K., 1969, Oxygen isotope fractionation in divalent metal carbonates: The Journal of Chemical Physics, v. 51, p. 5547–5558.

Parker, F. L., 1948, Foraminifera of the continental shelf from the Gulf of Maine to Maryland: Bulletin of the Museum of Comparative Zoology at Harvard College, v. 100, p. 213–241.

Peltier, W.R., 2004, Global glacial isostasy and the surface of the Ice-Age Earth: The ICE-5G (VM2) Model and GRACE: Annual Review of Earth and Planetary Sciences, v. 32, p. 111–149.

Peltier, W.R., and Fairbanks, R.G., 2006, Global glacial ice volume and Last Glacial Maximum duration from an extended Barbados sea level record: Quaternary Science Reviews, v. 25, p. 3322–3337.

Poag, W. C., Knebel, H. J., and Todd, R., 1980, Distribution of modern benthic foraminifers on the New Jersey Outer Continental Shelf: Marine Micropaleontology, v. 5, p. 43–69.

Rasmussen, C. E., and Williams, C. K., 2006, Gaussian Processes for Machine Learning: MIT Press, Cambridge, MA, 248 p.

Roarty, H., Cook, T., Hazard, L., George, D., Harlan, J., Cosoli, S., Wyatt, L., Alvarez Fanjul, E., Terrill, E., Otero, M., Largier, J., Glenn, S., Ebuchi, N., Whitehouse, B., Bartlett, K., Mader, J., Rubio, A., Corgnati, L., Mantovani, C., Griffa, A., Reyes, E., Lorente, P., Flores-Vidal, X., Saavedra-Matta, K. J., Rogowski, P., Prukpitikul, S., Lee, S.-H., Lai, J.-W., Guerin, C.-A., Sanchez, J., Hansen, B., and Grilli, S., 2019, The Global High Frequency Radar Network: Frontiers in Marine Science, v. 6. DOI: 10.3389/fmars.2019.00164.

Rothwell, R.G., 1989, Minerals and Mineraloids in Marine Sediments: An Optical Identification Guide, London, Springer Dordrecht, 282 p.

Schnitker, D., 1974, West Atlantic abyssal circulation during the past 120,000 years: Nature, v. 248, p. 385–387.

Streeter, S. S., 1973, Bottom water and benthonic foraminifera in the North Atlantic—Glacial-interglacial contrasts: Quaternary Research, v. 3, p. 131–141.

Swift, D. J. P., Stanley, D. J., and Curray, J. R., 1971, Relict sediments on continental shelves: A reconsideration: The Journal of Geology, v. 79, p. 322–346.

Swift, D. J. P., Duane, D. B., and McKinney, T. F., 1973, Ridge and swale topography of the Middle Atlantic Bight, Nnorth America: Secular response to the Holocene hydraulic regime: Marine Geology, v. 15, p. 227–247.

Twichell, D. C., Knebel, H. J., and Folger, D. W., 1977, Delaware River: Evidence for its former extension to Wilmington submarine canyon: Science, v. 195, p. 483–485.

Twichell, D. C., McClennen, C. E., and Butman, B., 1981, Morphology and processes associated with the accumulation of the fine-grained sediment deposit on the southern New England shelf: Journal of Sedimentary Petrology, v. 51, p. 269–280.

Uchupi, E., 1968, Atlantic Continental Shelf and Slope of the United States - Physiography: USGS Professional Paper, v. 529C, p. C1–C30.

van der Zwaan, G. J., Jorissen, F. J., and de Stigter, H. C., 1990, The depth dependency of planktonic/benthic foraminiferal ratios: Constraints and applications: Marine Geology, v. 95, p. 1–16.

Van der Zwaan, G. J., Duijnstee, I. A. P., den Dulk, M., Ernst, S. R., Jannink, N. T., and Kouwenhoven, T. J., 1999, Benthic foraminifers: Proxies or problems?: A review of paleocological concepts: Earth-Science Reviews, v. 46, p. 213–236.

Vaquer-Sunyer, R., and Duarte, C. M., 2008, Thresholds of hypoxia for marine biodiversity: PNAS, v. 105, p. 15452–15457.

Vilela, C. G., 1995, Ecology of Quaternary benthic foraminiferal assemblages on the Amazon shelf, northern Brazil: Geo-Marine Letters, v. 15, p. 199–203.

Williams, S. J., Arsenault, M. A., Poppe, L. J., Reid, J. A., Reid, J. M., and Jenkins, C. J., 2007, Surficial sediment character of the New York-New Jersey offshore continental shelf region: A GIS compilation, U.S. Geological Survey Report 2006-1046. DOI: 10.3133/ofr20061046.

Woehle, C., Roy, A.-S., Glock, N., Wein, T., Weissenbach, J., Rosenstiel, P., Hiebenthal, C., Michels, J., Schönfeld, J., and Dagan, T., 2018, A novel eukaryotic denitrification pathway in foraminifera: Current Biology, v. 28, p. 2536–2543.

Zhang, W. G., and Gawarkiewicz, G. G., 2015, Dynamics of the direct intrusion of Gulf Stream ring water onto the Mid-Atlantic Bight shelf: Geophysical Research Letters, v. 42, p. 7687–7695.

Received 18 August 2023
Accepted 8 February 2024